Planta (2007) 226:251–265
DOI 10.1007/s00425-006-0470-2

ORIGINAL ARTICLE

Metabolic processes and carbon nutrient exchanges between host and pathogen sustain the disease development during sunflower infection by *Sclerotinia sclerotiorum*

Cécile Jobic · Anne-Marie Boisson · Elisabeth Gout · Christine Rascle · Michel Fèvre · Pascale Cotton · Richard Bligny

Received: 24 October 2006 / Accepted: 15 December 2006 / Published online: 12 January 2007

Abstract Interactions between the necrotrophic fungus *Sclerotinia sclerotiorum* and one of its hosts, *Helianthus annuus* L., were analyzed during fungal colonization of plant tissues. Metabolomic analysis, based on ^{13}C- and ^{31}P-NMR spectroscopy, was used to draw up the profiles of soluble metabolites of the two partners before interaction, and to trace the fate of metabolites specific of each partner during colonization. In sunflower cotyledons, the main soluble carbohydrates were glucose, fructose, sucrose and glutamate. In *S. sclerotiorum* extracts, glucose, trehalose and mannitol were the predominant soluble carbon stores. During infection, a decline in sugars and amino acids was observed in the plant and fungus total content. Sucrose and fructose, initially present almost exclusively in plant, were reduced by 85%. We used a biochemical approach to correlate the disappearance of sucrose with the expression and the activity of fungal invertase. The expression of two hexose transporters, *Sshxt1* and *Sshxt2*, was enhanced during infection. A database search for hexose transporters homologues in the *S. sclerotiorum* genome revealed a multigenic sugar transport system. Furthermore, the composition of the pool of reserve sugars and polyols during infection was investigated. Whereas mannitol was produced in vitro and accumulated *in planta*, glycerol was exclusively produced in infected tissues and increased during colonization. The hypothesis that the induction of glycerol synthesis in *S. sclerotiorum* exerts a positive effect on osmotic protection of fungal cells and favors fungal growth in plant tissues is discussed. Taken together, our data revealed the importance of carbon–nutrient exchanges during the necrotrophic pathogenesis of *S. sclerotiorum*.

Keywords Acid invertase · *Helianthus* · Hexose transport · NMR spectroscopy · Polyols · *Sclerotinia*

Abbreviations

GPC	Glycerylphosphoryl-choline
GPE	Glycerylphosphoryl-ethanolamine
GPG	Glycerylphosphoryl-glycerol
GPI	Glycerylphosphoryl-inositol
hpi	Hours post-inoculation
PCA	Perchloric acid
PGA	Phosphoglyceric acid
Q-PCR	Quantitative polymerase chain reaction
UDP-GlcNAc	Uridine-5′-diphosphate-*N*-acetylglucosamine

C. Jobic · C. Rascle · M. Fèvre · P. Cotton (✉)
Laboratoire de Pathogénie des Champignons Nécrotrophes, CNRS, UMR5122, Unité Microbiologie et Génétique, Université Lyon 1, Bat Lwoff, 10 rue Raphaël Dubois, Villeurbanne, 69622, France
e-mail: cotton@biomserv.univ-lyon1.fr

A.-M. Boisson · E. Gout · R. Bligny
Laboratoire de Physiologie Cellulaire Végétale, Département Réponse et Dynamique Cellulaires, CEA-Grenoble, Université Joseph Fourier, UMR 5168, CEA, CNRS, INRA, 17 rue des Martyrs, Grenoble Cedex 9, 38054, France

Introduction

As a necrotrophic fungus, *Sclerotinia sclerotiorum* is able to feed on dead cells and is one of the most

non-specific and omnivorous plant pathogens (Boland and Hall 1994). Two main pathogenicity factors, secretion of oxalic acid and hydrolytic enzymes, act in concert to macerate plant tissues and generate necrosis. Degradation of plant cell wall components and host tissues is linked to the concerted production of a wide and complex range of extracellular lytic enzymes such as cellulases, hemicellulases, pectinases and proteases. Sequentially secreted by the fungus, lytic enzymes facilitate penetration, colonization and maceration but also generate an important source of nutrients (reviewed by Bolton et al. 2006). Secreted oxalic acid acidifies the apoplastic space, sequesters calcium, interferes with plant defenses and appears to be an essential determinant of pathogenicity (Maxwell and Lumdsen 1970; Hegedus and Rimmer 2005). The secretion of oxalic acid by *S. sclerotiorum* results in formation of lesions and water-soaked tissues, in advance of the invading fungal hyphae, rapidly expanding as a frontal zone of hosts cells impaired in their viability (Lumdsen and Dow 1973). To complete their life cycle *in planta*, pathogenic fungi must also be able to gain nutrients from plant cells.

Metabolic interactions between plants and fungi have been conducted on biotrophic and mycorrhizal fungi in most cases. Mycorrhizae are characterized by the uptake of minerals from the soil by fungal hyphae, followed by their transfer to the root cells. In return, plant carbohydrates are transferred to the fungal symbiont and their utilization is oriented towards the synthesis of short chain polyols (Martin et al. 1998; Bago et al. 1999). Free amino acids also represent an important sink of absorbed and assimilated carbon (Martin et al. 1998).

Biotrophs cause little damage to the host plant, and derive energy from living cells. They produce extensions into plant cells, haustoria, linked to maintain basic compatibility between fungi and their host plants and to nutrient uptake (Mendgen et al. 2000). During a compatible interaction, competition of the parasite with natural sink organs of the host, results in considerable modification of photoassimilate production and alterations in partitioning within host tissues (Scholes et al. 1994; Hall and Williams 2000; Abood and Lösel 2003). A common feature is a reduction in the rate of photosynthesis (Tang et al. 1996; Chou et al. 2000). During infection with *Albugo candida*, the decrease in photosynthesis was correlated with an accumulation of carbohydrates in leaves of *Arabidopsis thaliana* (Tang et al. 1996; Chou et al. 2000). Direct analysis of sugar composition of the leaf apoplast of tomato infected by *Cladosporium fulvum* indicated high levels of sucrose accumulated during early stages of infection that could be linked to the expression of plant or fungal invertases (Joosten et al. 1990). The induction of a sink-specific cell-wall invertase at the site of infection appears to be a general response to a biotic stress (Scholes et al. 1994; Fotopoulos et al. 2003; Roitsch et al. 2003; Voegele et al. 2006). Molecular analysis of compatible biotrophic interactions suggested that nutrients were mainly taken up in form of hexoses and amino acids, in accordance with the strong expression of amino acids and hexoses permeases in haustoria (Voegele et al. 2001; Struck et al. 2004). As shown for the compatible interactions *Uromyces fabae-Vicia faba* or *C. fulvum-Lycopsersicon esculentum*, much of the carbohydrates supplied to fungal biotrophic pathogens could be converted later in the infection cycle into the C6-polyol mannitol, that could play a pivotal role in suppression of ROS-related defence mechanisms or in carbon storage (Noeldner et al. 1994; Voegele et al. 2005).

The nature of available nutrient supplies metabolized by necrotrophic fungi during infection has received little attention up to now. Studies dedicated to carbohydrate and invertase activity changes during necrotrophic interactions are scarce and mainly focused on plant. Upon infection with *Botrytis cinerea*, photosynthetic gene expression was downregulated in tomato plant tissues and expression of a cell wall invertase was induced by the pathogen (Berger et al. 2004). Accumulation of invertase in the cell walls of tomato plants was induced by *Fusarium oxysporum* in susceptible and resistant hosts (Benhamou 1991). An elicitor preparation of the tomato pathogen *F. oxysporum* also activated invertase gene expression in tomato suspension culture cells (Sinha et al. 2002). In this study, we report a metabolic study of the necrotrophic interaction between *S. sclerotiorum* and cotyledonary leaves of sunflower based on NMR spectroscopy used to monitor cellular metabolism (Roberts and Jardetsky 1981; Shachar-Hill and Pfeffer 1996; Ratcliffe and Shachar-Hill 2001). In order to analyze metabolic processes that promote fungal development in plant tissues, we established the profiles of soluble metabolites for each partner and followed the quantitative modifications of these metabolites during the course of infection. Our results indicate a progressive exhaustion of plant carbohydrate stores in favor of the accumulation of glycerol of fungal origin. Fungal elements that could be linked to the decrease of plant sugars have been investigated. Increases of invertase activity and *in planta* expression of fungal hexose transporters are described.

Materials and methods

Fungal strain and growth conditions

S. sclerotiorum S5 was initially provided by Bayer-CropScience, Lyon, France. The strain was maintained on potato dextrose agar. For NMR characterization, mycelia were grown for 48 h on solid minimal medium (Riou et al. 1991) supplemented with 2% glucose. Mycelia were frozen in liquid nitrogen and stored at −80°C.

Pathogenicity tests

Phytopathogenicity assays were performed on sunflower cotyledons as hosts. Sunflower plants (*Helianthus annuus* L. variety Mirasol) were purchased from Limagrain (Riom, France). Sunflowers were grown at 25°C with a 14-h light period per day. Cotyledons from 1-week-old germlings were infected at the end of a dark period by depositing a 4-mm-mycelium disk at the center of the adaxial side. At 8 hpi (hours post-inoculation), mycelium discs were tightly attached to the surface of cotyledons, indicating the penetration of fungal hyphae into plant. Necrosis was detectable by the apparition of a brown color surrounding the starting point of infection. The necrosed and macerated region corresponded to a 2-mm-zone surrounding the mycelium discs 16 hpi. 24 hpi, half of the cotyledons were macerated and necrosed. At 48 hpi, the whole cotyledon was infected. Cotyledons were harvested after the different stages of symptoms development (8, 16, 24, 36, and 48 hpi). For invertase assays and some NMR experiments that were realized on fractions of infected cotyledons, plugs of mycelium were deposited near the tip of the leaves, in order to easily separate two distinct zones at different stages of infection: a non-invaded region and an invaded region. Absence of fungus was confirmed by microscope observation and by the absence of detected uridine-5′-diphosphate-*N*-acetylglucosamine (UDP-GlcNAc) in the spectra. Samples were then frozen in liquid nitrogen.

NMR spectroscopy

PCA extracts were prepared from 10 g of *H. annuus* cotyledons, or 10 g of *S. sclerotiorum* mycelia, or 10 g of infected cotyledons, according to the method described by Aubert et al. (1996). Spectra of neutralized PCA extracts were recorded in a Fourier transform NMR spectrometer (model AMX 400, Bruker Billerica MA) equipped with a 10-mm multinuclear probe tuned at 161.9 or 100.6 MHz for ^{31}P- or ^{13}C-NMR studies, respectively. The deuterium resonance of $^{2}H_2O$ (100 µl added per ml of extract) was used as a lock signal. ^{31}P-NMR acquisition conditions: 70° pulses (15-µs) at 3.6-s intervals; spectral width, 8.2 kHz; Waltz-16 ^{1}H decoupling sequence with 1 W decoupling during acquisition and 0.5 W during delay; free induction decays collected as 8,000 data points, zero-filled to 16,000, and processed with a 0.2-Hz exponential line broadening. Spectra were referenced to methylene diphosphonic acid, pH 8.9, at 16.38 ppm. Divalent paramagnetic cations were chelated by addition of corresponding amounts of 1,2-cyclohexylenedinitrilotetraacetic acid (CDTA).^{13}C-NMR acquisition conditions: 90° pulses (19-µs) at 6-s intervals; spectral width, 20 kHz; Waltz-16 ^{1}H decoupling sequence with 2.5 W decoupling during acquisition and 0.5 W during the delay; free induction decays collected as 32,000 data points, zero-filled to 64,000, and processed with a 0.2-Hz exponential line broadening. Spectra were referenced to hexamethyldisiloxane at 2.7 ppm. Mn^{2+} ions were chelated by addition of 1 mM CDTA. Assignments were made after running series of standard solutions of known compounds at pH 7.5 and after the addition of these compounds to PCA extracts as previously described (Aubert et al. 1996). Identified compounds were quantified by comparison of the surface of their resonance peaks to the surface of the resonance peaks of standards added to samples before grinding. Fully relaxed conditions during spectra acquisition (pulses at 20-s intervals) were used for quantification. The standards utilized were methyl phosphonate and maleate for ^{31}P- and ^{13}C-NMR analyses.

Preparation of protein extracts and detection of invertase activity

Frozen healthy plant material and infected plant tissues were ground to a fine powder in liquid nitrogen. Ground tissues were resuspended in cold extraction buffer (100 mM Tris pH 7.5, 2.5 mM EDTA, 5 mM DTT, 1 mM PMSF, 5 µg ml^{-1} pepstatin and 10 mM Chaps) and incubated 20 min at 4°C. Extracts were then centrifuged at 13,000*g* for 30 min at 4°C. Supernatants containing total proteins were collected and stored at −20°C. Secreted proteins from in vitro culture filtrates were concentrated by $(NH_4)_2SO_4$ precipitation (80% saturation) overnight at 4°C. After centrifugation at 12,000*g* for 30 min at 4°C, the proteins present in pellets were dissolved in distilled water and stored at −20°C. Protein concentration was determined using the BioRad protein Assay (BioRad, Marnes la Coquette, France), with BSA as the standard.

Proteins (10 μg) extracted from healthy and infected tissues or recovered from culture filtrates were separated by isoelectric focusing (IEF) using ultrathin polyacrylamide gels (Servalyt Precotes, pH 3–10, Serva Heidelberg, Germany). Gels were focused for 1.5 h at 3 W, 1,700 V and 1 mA. A part of the slab gel was stained with Coomassie brillant blue for protein visualization, the other part was used to reveal invertase activities by zymography, according to Chen et al. (1996). After electrophoresis, gels were covered by a 1% agarose overlay containing 500 mM sucrose in 50 mM sodium acetate pH 5.6 or 4 or in 50 mM Hepes buffer pH 7, at 30°C for 30 min. Invertase isoforms were revealed by incubating the gels in 1% 2,3,5-triphenyltetrazolium chloride monohydrate (Sigma, St Quentin-Fallavier, France) in 0.25 M hot NaOH. Red color development was stopped with 1% acetic acid.

Immunological methods

Proteins (10 μg) were separated by SDS polyacrylamide gel electrophoresis (SDS PAGE) according to Laemmli (1970), using the miniprotean-2D system (BioRad, Marnes la Coquette, France). After migration in a 7% acrylamide gel, proteins were blotted onto nitrocellulose (Schleicher and Schuell Gmbh, Dassel, Germany) according to Towbin et al. (1979). Nitrocellulose membranes were incubated for 2 h at room temperature in 5% non-fat dry milk, 150 mM NaCl, 50 mM Tris–HCl pH 7.4, 0.01% Tween 20, rinsed in 150 mM NaCl, 50 mM Tris–Hcl pH 7.4, 0.05% Tween 20 and then incubated 1 h in the presence of antisera. Primary antisera were used at a dilution of 1:5,000. Antisera raised against tobacco cell wall invertase were kindly provided by Dr S. Greiner (Heidelberger Institut für Pflanzenwissenschaften, Germany). Antisera raised against *Candida albicans* invertase were purchased from USBiological (Euromedex, Mundolsheim, France). Incubations with anti-rabbit IgGs (anti-tobacco invertase, 1:20,000 and anti-*C. albicans* invertase, 1:2,000) was followed by detection using enhanced chemiluminescent substrate (Pierce Super Signal Substrate, Pierce Perbio-France, Brebières, France). Cross reactivity of the antisera was tested. No proteins from healthy plant tissues extracts were detected by anti fungal antisera. As well, antiplant antisera did not detect any protein extracted from the mycelium of *S. sclerotiorum* or secreted by the fungus.

Cloning *Sshxt1* and *Sshxt2* genes

EST sequences (BfCon 1401(and BfCon(1411)) from the related necrotrophic fungus *Botrytis cinerea*, deposited in the public databases (COGEME phytopathogen EST databases, http://www.cogeme.ex.ac.uk/) as putative hexose transporters (Soanes et al. 2002), were used as probes to screen at low stringency the genomic EMBL3 library of *S. sclerotiorum*. For *Sshxt1*, a 205-bp *B. cinerea* genomic DNA fragment was amplified using the sense primer 5′-GAATTGTCTTTG CTTGCCTC-3′ and the antisense primer 5′-TGGGGT GAAGAATGCAAG-3′. For *Sshxt2*, the sense primer 5′-GATCTTGGGTCTGCGATGAC-3′ and the antisense primer 5′-CTGGTGCCGTTCTTATCTG-3′ were used to amplify a 300-bp *B. cinerea* genomic DNA. 25 ng of *B. cinerea* genomic DNA were used as template. PCR conditions were as follows: after denaturation at 94°C for 5 min, annealing of the primers was done at 54°C to amplify the probe used to clone *Sshxt1* and at 60°C to amplify the probe used to clone *sshxt2*. After an extension step at 72°C for 1 min, a final elongation step at 73°C for 8 min was added for 30 cycles. Each amplified fragment was sequenced and used to screen the library at low stringency (37°C, 50% formamide, 5 SSC). One recombinant phage giving the strongest hybridization signal for each gene was chosen for further studies. Subcloning and routine procedures were performed with standard protocols (Sambrook 1989). Sequences of *Sshxt1* and *Sshxt2* are available in GenBank under the following accession no.: AY647267 and AY647268 respectively.

RNA isolation and Q-PCR

RNA was extracted from plant material frozen in liquid nitrogen and kept at −80°C. Samples were ground in liquid nitrogen, and total RNA was purified by using RNeasy mini spin column as described by manufacturers (Qiagen, Courtabeuf, France). Transcripts of *Sshxt1* were amplified using the sense primer 5′-GGTG TCGAAGAATCCCATCCA-3′ and the antisense primer 5′-GTGCTGGCAAAACCGACGAT-3′. Transcripts of *Sshxt2* were amplified using the sense primer 5′-ACTACTATGTGCTTGTCTTTGC-3′ and the antisense primer 5′-GATGCTGCTTCCCAAACG CCATTA-3′. To detect transcripts of the *S. sclerotiorum* actin gene *Ssact1*, the sense primer 5′-CTTCGTG TAGCACCAGAGGA-3′ and the antisense primer 5′-ATGTTACCATACAAATCCTTA-3′ were used. For quantitative polymerase chain reaction (Q-PCR) analysis, total RNA was DNaseI treated (RQ1 RNase free DNase, Promega, Charbonnières, France) to remove genomic DNA. Absence of DNA was analyzed by performing a PCR reaction similar to the real-time PCR program, on the DNaseI-treated RNA using Taq-DNA polymerase (Promega, Charbonnières, France).

Q-PCR experiments were performed using the one-step QuantiTect SYBR Green RT-PCR kit (Qiagen, Courtabeuf, France) according to the instructions of the manufacturer. Reactions were performed in a final volume of 20 µl, using 1 µg of total RNA, 1 µM of each primer, 10 µl of QuantiTec SYBR Green RT-PCR Master Mix (containing Hot Start Taq DNA polymerase, QuantiTect SYBR Green RT-PCR buffer, dNTP mix, SYBR Green and 5 mM MgCl2). The amplification was effected in the LightCycler (Roche, Meylan, France). The following amplification program was used: 20 min at 50°C for cDNA synthesis, 15 min at 95°C to activate the Hot Start DNA polymerase and 45 cycles of amplification as follows: 15 s at 94°C, 30 s at 60°C for *Sshxt1*, 54°C for *Sshxt2* and 60°C for *Ssact1* and 30 s at 72°C. Relative quantification was based on the C_T method using *Ssact1* as a calibrator reference. Amplifications were done in triplicate.

Results

Metabolic characterization of plant and fungal pathogen

Perchloric acid (PCA) extracts of healthy cotyledonary leaves collected from 8-d-old *H. annuus* germlings and of *S. sclerotiorum* mycelia collected after saprophytic growth on minimal glucose medium were analyzed using ^{13}C- and ^{31}P-NMR spectroscopy. Representative spectra are shown in Figs. 1 and 2, and comparative data are given in Table 1.

In *H. annuus* cotyledon extracts, the main stores of soluble carbohydrates detected by ^{13}C-NMR (Fig. 1) were glucose, fructose and sucrose (63, 40 and 11 µmol g^{-1} FW of plant tissues, respectively). Plants do not accumulate trehalose. Inositol (10 µmol g^{-1} FW) was the only detected polyol. The most abundant Krebs cycle intermediates were fumarate, malate, succinate and citrate. Glutamate (18 µmol g^{-1} FW) was the main amino acid store. The concentration of alanine, the second unambiguously identified amino acid, was 18 times lower. The most abundant compound measured by ^{31}P-NMR (Fig. 2b) was inorganic phosphate (2.5 µmol g^{-1} FW). Among identified P-compounds (from upfield to downfield): glucose−6-P, glycerol-3-P, phosphoglyceric acid (PGA), P-choline, two phosphodiesters, glycerylphosphoryl-glycerol (GPG) and glycerylphosphoryl-inositol (GPI) were detected. Nucleotides (mainly ATP), pyridine nucleotides (NAD and NADP), UDP-glucose and UDP-galactose were also detected. The abundance of GPG and GPI may be related to membrane traffic accompanying the first steps of growth of the germlings (Aubert et al. 1996).

In *S. sclerotiorum* extracts, main stores of soluble carbohydrates (Fig. 1) were glucose (115 µmol g^{-1} FW) and trehalose (26 µmol g^{-1} FW). Contrary to *H. annuus*, fructose and sucrose stores were negligible in *S. sclerotiorum*. Mannitol (27 µmol g^{-1} FW) was the only abundant polyol, while glycerol, arabitol and erythritol, commonly found in other fungi (Jennings 1984) were below the threshold of ^{13}C-NMR detection. Malate and fumarate were the two main stores of Krebs cycle intermediates. Like in *H. annuus* cotyledons, glutamate (17 µmol g^{-1} FW) was the main store of amino acid. Alanine (8.0 µmol g^{-1} FW) was eight times more abundant than in plant. Here again, the most abundant compound measured by ^{31}P-NMR (Fig. 2a) was inorganic phosphate (2.7 µmol g^{-1} FW). Glucose−6-P, PGA, ATP, UDP-glucose and UDP-galactose were equally detected in mycelium and in plant tissues. In contrast, there were striking differences concerning UDP-GlcNAc, trehalose-6-P, gluconate-6-P, P-choline and phosphodiesters. UDP-GlcNAc was the major P-compound in mycelium (1.4 µmol g^{-1} FW) whereas it was only present as a trace in cotyledons. In fungi, UDP-GlcNAc is predominantly involved in the synthesis of chitin, a structural constituent carbohydrate polymer of cell wall and septum with glucans (Cabib et al. 1991). Similarly, trehalose-6-P, which was not detected in cotyledons, was relatively abundant in mycelium (0.19 lmol g¡1 FW), in accordance with the presence of trehalose. Glycerylphosphoryl-choline (GPC) and glycerylphosphoryl-ethanolamine (GPE) were the most abundant P-diesters. Interestingly, though glycerol-3-P was present in both partners grown in vitro, glycerol was detected in none of them.

Metabolic profiling during infection

As control experiments, we first verified that the NMR profiles of non-infected cotyledons, maintained in the same growth conditions as inoculated cotyledons for a 48 h period of time equivalent to the course of infection, did not change significantly. Moreover, NMR spectra of samples collected 0 hpi were realized. At the initial stage of infection, the major components from fungal origin (UDP-GlcNAc, mannitol, trehalose) were not detectable. Analysis of the spectra revealed profiles identical to that of healthy cotyledons profiles. On the contrary, ^{13}C- and ^{31}P-NMR spectra of *H. annuus* cotyledons infected by *S. sclerotiorum* revealed that the interaction induced changes in the

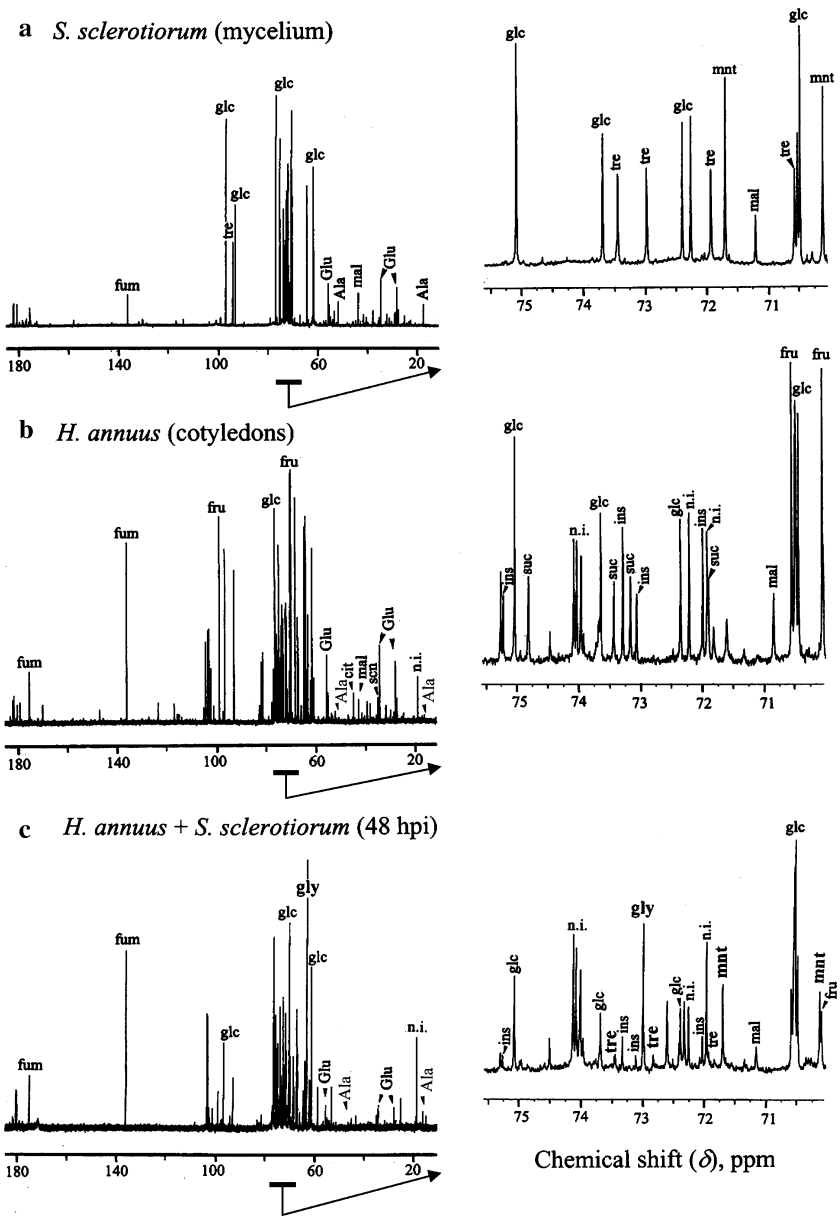

Fig. 1 ^{13}C-NMR spectra of *S. sclerotiorum* mycelium (**a**), *H. annuus* cotyledon (**b**) and sunflower cotyledons infected by *S. sclerotiorum* 48 hpi (**c**). Perchloric extracts were prepared from 10 g fresh material as described in Materials and methods. ^{13}C-NMR spectra (100.6 MHz), recorded at 20°C, were the result of 900 transients (90 min). Peak assignments are as follows: *Ala* alanine, *cit* citrate, *fru* fructose, *fum* fumarate, *glc* glucose, *Glu* glutamate, *gly* glycerol, *ins* inositol, *mal* malate, *mnt* mannitol, *n.i.* not identified, *scn* succinate, *suc* sucrose, *tre* trehalose. Prominent fungal compounds are indicated in *bold* in panel (**c**). Panels on the right show a focused region of each spectra

composition of the pool of soluble metabolites (Figs. 1, 2 and Table 1). A decrease in sugars and amino acids was observed. The total carbohydrate level was only 59 and 57 μmol g^{-1} FW of infected tissues, 24 and 48 hpi, whereas it was 125 and 179 μmol g^{-1} FW in plant and fungal tissues, respectively. More specifically, fructose and sucrose, initially present almost exclusively in plant, were reduced by 85%. These results suggest that plant carbohydrate stores were utilized for fungal growth.

Analyses of ^{13}C-NMR spectra also revealed changes in the composition of the pool of storage carbohydrates: inositol, the plant polyol marker, decreased from 10 to 2.1 μmol g^{-1} FW of infected tissues 48 hpi (Fig. 1 and Table 1). Trehalose, a specific fungal carbohydrate remained constant during infection, whereas the level of mannitol, the main fungal polyol, revealed a fourfold increase from 24 to 48 hpi. This may suggest that trehalose did not constitute the main carbohydrate endogenous store in fungus, whereas mannitol was actively produced. The accumulation of glycerol in infected cotyledons was more surprising since this polyol was detected neither in plant nor in fungus cultivated separately. During infection, free glycerol increased steadily, reaching 23–25 μmol g^{-1} FW 48 hpi. Additional experiments indicated that *S. sclerotiorum* accumulated glycerol but not mannitol as compatible osmolyte, when cultivated for 24 h in a hyper-osmotic medium containing 0.4 M NaCl (data not shown). Therefore, glycerol synthesis could occur in reaction to

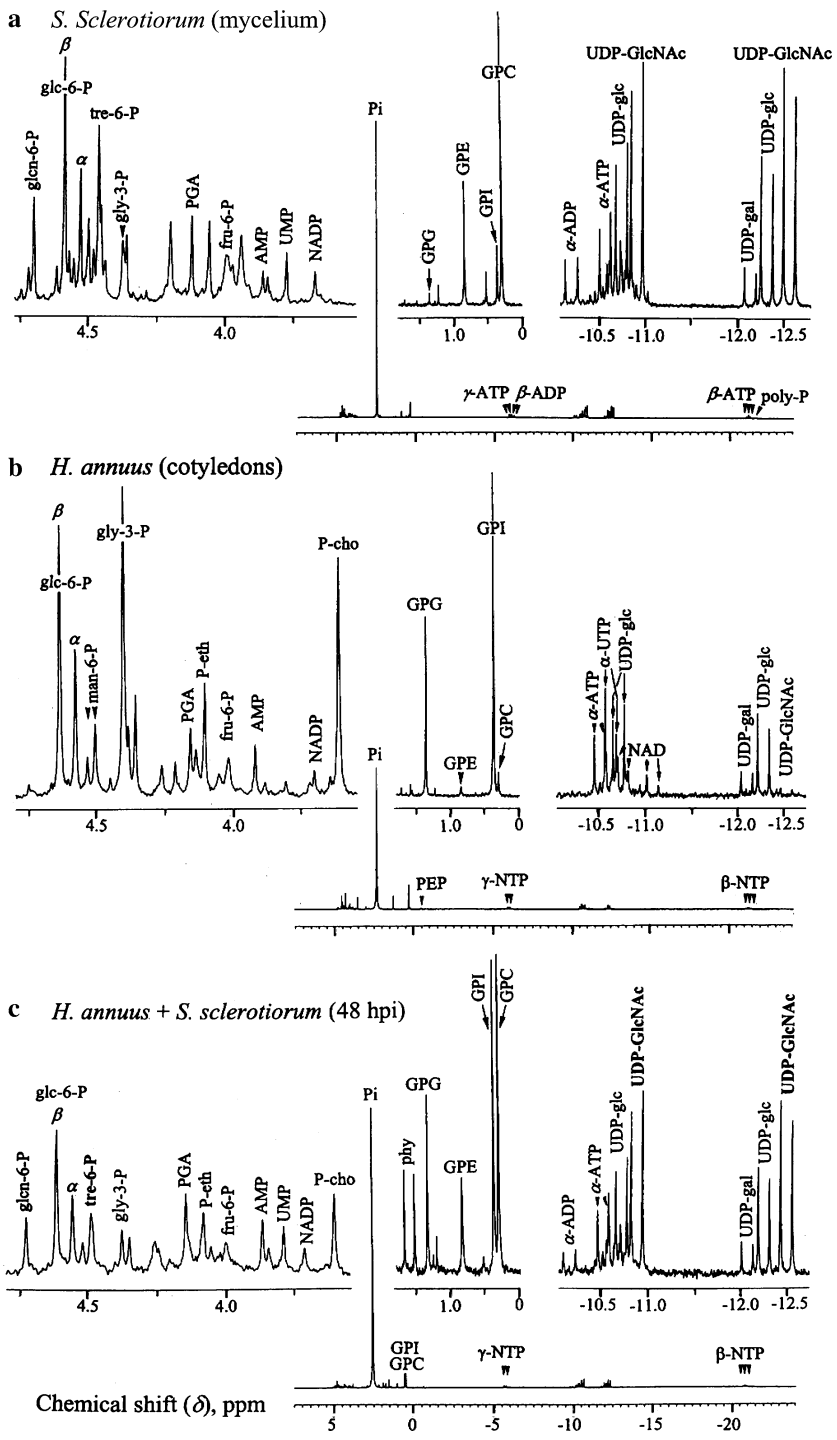

Fig. 2 Proton-decoupled in vitro ^{31}P-NMR spectra of *S. sclerotiorum* mycelium (**a**), *H. annuus* cotyledon (**b**) and sunflower cotyledons infected by *S. sclerotiorum* 48 hpi (**c**). Perchloric extracts were prepared from 10 g fresh material as described in Materials and methods. Spectra (161.9 MHz) recorded at 20°C were the result of 1,024 transients (60 min). Peak assignments are as follows: *fru-6-P* fructose-6-phosphate, *glcn-6-P* gluconate-6-P, *glc-6-P* glucose-6-P, *gly-3-P* glycerol-3-P, *man-6-P* mannose-6-phosphate, *P-cho* phosphorylcholine, *PEP* phosphoenolpyruvate, *P-eth* phosphorylethanolamine, *phy* phytate, *Pi* inorganic phosphate, *poly-P* polyphosphates, *tre-6-P* trehalose-6-P, *UDP-glc* UDP-glucose, *UDP-gal* UDP-galactose. The internal reference is not shown. Spectra are representative of three independent experiments. Prominent fungal compounds are indicated in *bold* in **c**

osmolarity changes possibly associated to the release of metabolites by dying plant cells or contribute to the osmotic stabilization of the hyphae required for invasive growth through tissues of living plants.

Glutamate and alanine, the two main free amino acids of plant or fungal origin, were detected in infected cotyledons at 24 and 48 hpi. Glutamate, initially abundant both in plant and mycelium, decreased strongly during the first hours of infection (data not shown), reaching less than 10% of the initial values 24 hpi, then increasing to 22% 48 hpi. Alanine, initially much more abundant in mycelium, accumulated moderately throughout the development of infection (Fig. 1 and Table 1).

Carbohydrate and amino acid storage in cotyledons was also affected at distance during fungal infection. For example, 40–50% decrease in glucose, fructose, sucrose and glutamate was observed 24 hpi

Table 1 Metabolic profiling of *S. sclerotiorum* mycelium, *H. annuus* healthy cotyledons and infected cotyledons collected 24 and 48 hpi

Metabolite	Healthy cotyledons	Infected cotyledons (24 hpi)	Infected cotyledons (48 hpi)	*S. sclerotiorum* mycelium
Total carbohydrate	125 ± 10	59 ± 5	57 ± 5	179 ± 12
Glucose	63 ± 5	35 ± 3	50 ± 4	115 ± 12
Fructose	40 ± 4	20 ± 2	7.0 ± 0.6	2.3 ± 0.2
Sucrose	11 ± 1	2.1 ± 2	n.d.	<1.0
Trehalose	n.d.	1.3 ± 0.2	1.0 ± 0.02	26 ± 3
Glycerol	n.d.	4.4 ± 0.3	24 ± 2	n.d.
Inositol	10 ± 1	3.3 ± 0.3	2.1 ± 0.2	n.d.
Mannitol	n.d.	1.3 ± 0.2	5.6 ± 0.6	27 ± 3
Malate	6.8 ± 0.5	7.2 ± 0.4	2.4 ± 0.2	12 ± 1
Succinate	3.5 ± 0.3	3.7 ± 0.3	1.2 ± 0.2	1.0 ± 1
Citrate	2.5 ± 0.2	3.5 ± 0.3	1.2 ± 0.2	n.d.
Fumarate	23 ± 2	27 ± 2	23 ± 2	6.0 ± 1
Glutamate	18 ± 2	1.9 ± 0.2	4.0 ± 3	17 ± 2
Alanine	1.0 ± 0.2	<1.0	2.4 ± 0.2	8.0 ± 1
Pi	2.5 ± 0.2	2.1 ± 0.2	2.90 ± 0.3	2.7 ± 0.3
Glucose-6-P	0.86 ± 0.06	0.78 ± 0.6	0.63 ± 0.5	1.2 ± 0.1
Trehalose-6-P	n.d.	0.07 ± 0.02	0.14 ± 0.015	0.55 ± 0.05
Glycerol-3-P	0.67 ± 0.05	0.12 ± 0.01	0.16 ± 0.015	0.19 ± 0.02
PGA	0.13 ± 0.02	0.2 ± 0.02	0.2 ± 0.02	0.23 ± 0.02
P-choline	0.50 ± 0.04	0.39 ± 0.04	0.23 ± 0.03	n.d.
GPG	0.54 ± 0.04	0.45 ± 0.04	0.38 ± 0.04	<0.04
GPE	<0.04	0.06 ± 0.01	0.21 ± 0.02	0.37 ± 0.04
GPI	0.98 ± 0.07	0.72 ± 0.06	0.68 ± 0.06	0.18 ± 0.015
GPC	0.07 ± 0.01	0.31 ± 0.03	0.68 ± 0.06	0.90 ± 0.07
ATP	0.16 ± 0.015	0.18 ± 0.02	0.18 ± 0.02	0.35 ± 0.03
NAD	0.08 ± 0.01	n.d.	n.d.	0.04 ± 0.01
NADP	0.055 ± 0.006	n.d.	n.d.	0.12 ± 0.01
UDP-Glc	0.25 ± 0.03	0.22 ± 0.03	0.35 ± 0.04	0.89 ± 0.07
UDP-GlcNAc	<0.04	0.29 ± 0.03	0.57 ± 0.05	1.4 ± 0.12

Metabolites are identified and quantified from a series of experiments, using maleate and methylphosphonate as internal standards for ^{13}C- and ^{31}P-NMR, respectively, as indicated in Materials and methods. Values are given as μmol g^{-1} FW. Results are given as mean ± SD (n = 3)

n.d. not detected

in the non-invaded region of leaves, beyond the infected area (data not shown). This suggests that the fungus behaves as a sink towards the metabolites required for its own growth, at the expense of plant stores.

^{31}P-NMR spectra first showed the appearance of tre-6-P and a dramatic increase of UDP-GlcNAc, reflecting the rapid proliferation of fungal hyphae in infected cotyledons tissues. The concentration of GPC in infected tissues increased simultaneously, reaching the one of GPI (Fig. 2). Accumulation of GPC in plant cells often reveals a stress, leading to partial hydrolysis of phospholipids (Aubert et al. 1996). Thus, its increase in infected tissues could indicate that fungal invasion gave rise to plant membrane systems hydrolysis and to subsequent release of metabolites in the apoplast. As GPC is the most abundant phosphodiester in *S. sclerotiorum* mycelium (Table 1), its presence in infected cotyledons may also reflect fungal growth in plant tissues.

Detection of invertase in infected cotyledons

Analysis of ^{13}C-NMR spectra revealed that sucrose, present exclusively in plant, decreased from 11 to 2.1 μmol g^{-1} during the first 24 hpi and was not detectable 48 hpi. The disappearance of sucrose from infected sunflower cotyledons could likely be correlated with an increase of invertase activities. In order to discriminate between the induction of fungal activity or plant enzymes activated in response to the fungal attack, we used a biochemical approach to investigate the presence of invertase during infection. Plants contain different isoforms of invertases, which can be distinguished by their subcellular location and biochemical properties (Godt and Roitsch 1997). To assess an invertase enzymatic activity *in planta*, proteins were extracted from healthy and infected sunflower cotyledons. Except for 0 and 48 hpi, infected tissues were separated in two regions: healthy tissues not colonized (region a) and invaded tissues (region

b). Proteins were separated by IEF over a pH range of 3–10. Invertase activity was revealed at pH 5.6 and visualized by staining reducing sugars in the gel. Two isoforms (pI 4 and 4.5) were detected (Fig. 3a). Invertase activity associated to the protein with pI of 4.5 was detected in healthy sunflower cotyledons and remained constant until 24 hpi. Thereafter, plant tissues were totally macerated. On the contrary, the presence of the invertase isoform with a pI of 4 was correlated with the presence of the fungus in the infected plant. Invertase activity was hardly detectable 8 hpi (region 8b), then increased strongly at 24 hpi (region 24b) and 48 hpi. Detection of invertase activity was also performed at pH 4 and 7 and revealed, at a lower level, the same pattern of activity for the protein with a pI of 4, while no activity was detected at pH 4 and 7 for the isoform with a pI of 4.5 (data not shown). This indicates that the activities of both enzymes were detected using favorable pH conditions. In order to reveal the fungal or plant origin of the major invertase activity detected at a pI of 4, we used immunospecific detection. Western-blot analyses (Fig. 3b, c) revealed two isoforms, differing in their molecular weight and separately detected by antibodies raised against a fungal invertase (Fig. 3b) and a plant cell wall invertase (Fig. 3c). A 81 kDa isoform was abundantly detected by anti-fungal invertase antibodies and its presence was limited to regions severely colonized by *S. sclerotiorum* (24b and 48 hpi). The 40 kDa isoform, detected by anti-plant invertase antibodies exhibited a different pattern and was present in healthy tissues and during infection during the first 24 hpi. This isoform was not detected 48 hpi when sunflower cotyledons were completely invaded and macerated. This protein was consequently not linked to the fungus but rather correlated with the presence of healthy plant tissues. The presence of the 81 kDa isoform paralleled the invertase activity detected at pI 4 and could likely be attributed to the fungus. Analyses of biochemical properties of the fungal invertase expressed during in vitro growth in the presence of 10 mM sucrose, confirmed our suggestions. Figure 3d revealed an unique active isoform at pI 4, released in the culture medium by *S. sclerotiorum* during 36 h growth in the presence of sucrose, that corresponds to the isoform detected in plant tissues (Fig. 3a). Moreover, Western-blot analyses conducted with proteins of the same origin and anti-fungal invertase antibodies (data not shown), revealed a band of 81 kDa, corresponding to the isoform detected *in planta* (Fig. 3b). These results strongly suggested that the major acid invertase activity detected during infection was mainly of fungal origin.

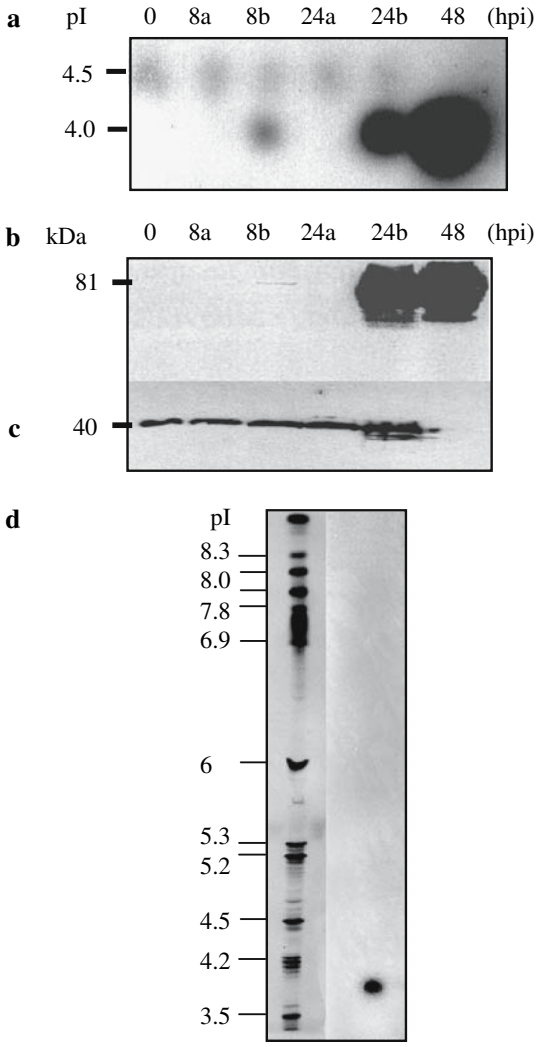

Fig. 3 Detection of soluble invertase in planta and in vitro. All lanes were loaded with 10 µg. For *lanes 8a*, *8b*, *24a*, and *24b* infected cotyledons were cut in half. *Lanes 8a* and *24a* correspond, respectively, to healthy regions of infected cotyledons 8 and 24 hpi, *lanes 8b* and *24b* correspond to regions colonized by *S. sclerotiorum* 8 and 24 hpi. Samples were prepared on an equal leaf area. **a** Isoelectrofocusing pattern of invertase produced during the time course of infection of sunflower cotyledons by *S. sclerotiorum*. Invertase activity was visualized by staining reducing sugars with TTC after incubation at pH 5.6. **b, c** Immunospecific detection of plant and fungal invertases in infected sunflower cotyledons extracts revealed respectively with anti-*C. albicans* invertase and anti-tobacco invertase. **d** Isoelectrofocusing pattern of *S. sclerotiorum* invertase produced after 36 h of growth on 10 mM sucrose medium. *Lane 1* protein standards stained with Coomassie blue, *lane 2* invertase activity revealed as in section (**a**). Western blots and IEFs were repeated at least twice

Expression of fungal hexose transporters during infection

Pathogenic fungi must feed on their hosts. During pathogenesis of sunflower cotyledons, plant stores and

particularly carbohydrates are likely transferred in the fungal mycelium, which suggests that the fungal plasma membrane is equipped with corresponding transporters. Thus, two genes *Sshxt1* and *Sshxt2*, encoding hexose transporters from *S. sclerotiorum*, have been isolated. For this purpose, EST sequences from the related necrotrophic fungus *B. cinerea*, identified in public databases (Soanes et al. 2002) and showing several convincing matches to fungal hexose transporters were used as probes to screen at low stringency the genomic EMBL3 library of *S. sclerotiorum*. Two recombinant phages giving the strongest hybridization signals were chosen for further studies. Restriction and Southern analyses allowed to clone and to characterize two sequences of 2,133 and 2,099 bp containing the coding sequences of *Sshxt1* and *Sshxt2*, respectively. Each sequence had two introns. SsHXT1 and SsHXT2 possess 12 membrane-spanning domains (Fig. 4) characteristic for members of the major facilitator super family (Marger and Saier 1993). The GRR or GRK conserved regions are implicated in the membrane topology of this group of transporter proteins (Sato and Mueckler 1999). Sequences analyses and databases searches revealed that SsHXT1 and SsHXT2 contain a five-element fingerprint that provides a signature for the sugar transporter family of membrane proteins (InterProScan, Zdobnov and Apweiler 2001). The presence of a conserved Phe residue, situated in the transmembrane domain X, implicated in the specificity of the transport, was also detected in all sequences (Özcan and Johnston 1999). Highly conserved regions identified within the fructose transporters as fungal fructose-proton symporter signatures and found in BcFRT1, a fructose transporter present in *B. cinerea* (Doehlemann et al. 2005), were not detected in SsHXT1 and SsHXT2 sequences. Thus, SsHXT1 and SsHXT2 contain the main sugar transport signatures but are probably not sole fructose transporters.

Recently, the release of the genome sequence of *S. sclerotiorum* (http://www.broad.mit.edu) offered new opportunities to identify sugar transporters sequences. A Blast search for possible homologies with SsHXT1 revealed, for the first hits, at least six additional sequences. These proteins belong to the family of membrane proteins responsible for the transport of sugars, as revealed by the InterProScan database (Zdobnov and Apweiler 2001). To illustrate the relatedness of these and other sequences, a dendrogram was generated (Fig. 5). Sugar transport sequences do not form a uniform group. It clearly showed that SsHXT1 and SsHXT2 clustered together (46% identity to each other) and were related to ApHXT1, an *A. parasiticus* monosaccharide transporter (Yu et al. 2000) with 30.3 and 34.3% identity, respectively. Five other sequences were more related to the *N. crassa* glucose sensors NcRCO3 (Madi et al. 1997) and the monosaccharide transporter AmMSTA (Nehls et al. 1998), a candidate gene encoding a homologue to the glucose sensors Rgt2 and Snf3 in *Saccharomyces cerevisiae* (Wei et al. 2004). Among these five sequences, three (SsIG-028441, SsIG-066201 and SsIG-084251) were predicted to be high-affinity transporters by the databases (InterProscan, Zdobnov and Apweiler 2001), whereas a separated branch contained a *B. cinerea* fructose transporter and one *S. sclerotiorum* putative hexose transport sequence (Ss1G-030921).

In planta expression of *Sshxt1* and *Sshxt2* genes was analyzed. Relative levels of *Sshxt1* and *Sshxt2* mRNAs were determined using real-time Q-PCR (Fig. 6). In these experiments, mRNA level for the stably expressed fungal gene encoding actin *Ssact1*, was evaluated as control gene for Q-PCR analyses. Total

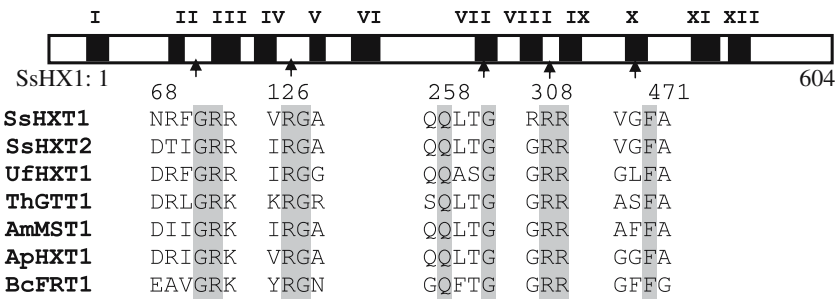

Fig. 4 Conserved amino acid stretches for fungal monosaccharide transporters. Locations of the conserved sequences, in SsHXT1 and SsHXT2, are indicated by numbering above the SsHXT1 sequence. Residues conserved in all seven transporters homologues are shaded in gray. *Black bars* indicate transmembrane domains of SsHXT1. Conserved domains were deduced from the alignment of the following protein sequences obtained by using the CLUSTALW algorithm and are positioned by *arrows* on the SsHXT1 sequence. Abbreviations and accession numbers are as follows: *S. sclerotiorum* SsHXT1 (AY647267), *S. sclerotiorum* SsHXT2 (AY647268), *U. fabae* UfHXT1 (AJ310209), *T. harzianum* ThGTT1 (AJ269534), *A. muscaria* AmMST1 (ZZ83828), *A. parasiticus* ApHXT1 (AF010145), *B. cinerea* BcFRT1 (AY738713)

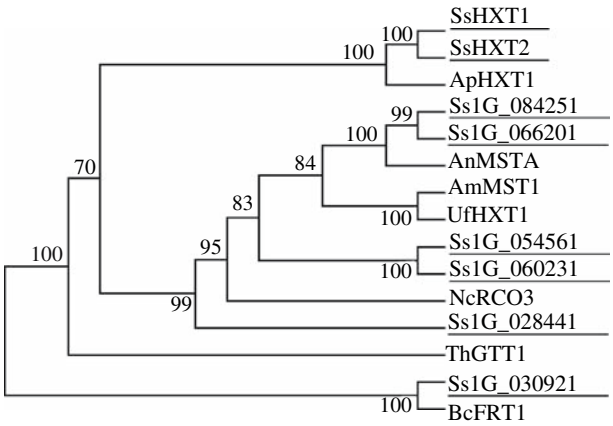

Fig. 5 Phylogram of hexose transporters-related proteins from *S. sclerotiorum* and other fungi. Consensus tree prediction was performed by using multiple sequence alignment, by cluster algorithms with the TreeTop-Phylogenetic Tree prediction program (GenBee). Numbers represent the percentage of occurrence obtained after bootstrap analysis (1,000 random samples) of the phylogenetic tree. Abbreviated species names are as indicated in Fig. 4 and as follows: *N. Crassa* RCO3 (accession no. U54768), *A. nidulans* AnMSTA (accession no. AJ535663). Other putative *S. sclerotiorum* sequences (Ss1G_084251, Ss1G_066201, Ss1G_054561, Ss1G_060321, Ss1G_028441, Ss1G_030921) are predicted proteins obtained from the *Sclerotinia sclerotiorum* Sequencing Project, Broad Institute of Harvard and MIT (http://www.broad.mit.edu) according to InterProScan databases (Zdobonov and Apweiler 2001). Sequences from *S. sclerotiorum* are *underlined*

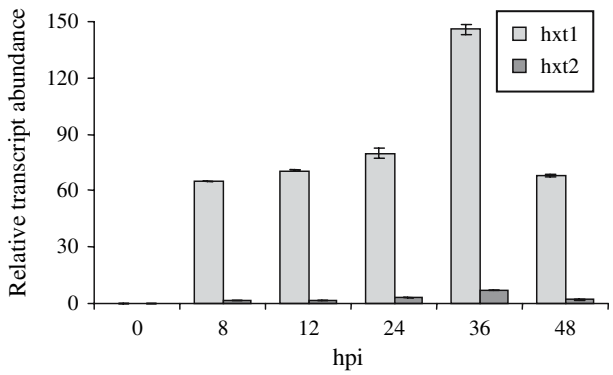

Fig. 6 Relative *Sshxt1* and *Sshxt2* expression analyzed by Q-PCR during time course of sunflower cotyledon infection. Relative expression levels were normalized with respect to *Ssact1* expression levels

mRNAs were extracted from infected tissues collected 8, 12, 24, 36 and 48 h after inoculation. Analysis of the expression profiles of *Sshxt1* and *Sshxt2* revealed wave expression patterns with a maximum of transcripts reached 36 hpi. Expression levels of *Sshxt1* and *Sshxt2* were not similar. *Sshxt1*, contrary to *Sshxt2*, was highly expressed during infection. The high level of expression of *Sshxt1* suggested that this gene is predominantly implicated in hexose transport during pathogenesis of sunflower cotyledons.

Discussion

This study reports on metabolic profiles of a necrotrophic interaction between the widespread pathogen *S. sclerotiorum* and sunflower cotyledons as host plant. For this purpose, the NMR spectroscopy offered an elegant way to build up a foundation of metabolic information about nutrition of a necrotroph fungal pathogen during infection.

Analyses of the natural abundance spectra revealed the progressive exhaustion of plant carbohydrates stores like sucrose and fructose. Simultaneously, fungal activities implicated in sucrose degradation and hexose transport were expressed. Upon compatible interactions of plants with pathogenic fungi, plant carbohydrate metabolism is affected. An increase in extracellular invertase activity, the inverse regulation of photosynthesis and carbohydrates withdraw from the plant by the pathogen, creates a sink which reflects the switch from normal metabolism to defense metabolism (Roitsch et al. 2003). The precise origin of the increase in invertase activity remains controversial, as both host and pathogen possess soluble and insoluble invertases. Therefore, it is difficult to establish whether the invertase activity stimulation is due to activation or to an increase in the amount of host proteins, or to a fungal invertase. The major plant invertases activated during a compatible interaction with biotrophic fungi are described as acid insoluble (cell wall-bound) enzymes (Benhamou et al. 1991; Scholes et al. 1994; Fotopoulos et al. 2003; Voegele et al. 2006). Acid soluble (vacuolar) and cytoplasmic invertase isoforms do not exhibit a major increase of their expression during biotrophic interactions, but are thought to be implicated in the metabolism of stored plant sucrose (Roitsch et al. 2003; Voegele et al. 2006). Our study elucidated the origin of the invertase activity detected in tissues infected by *S. sclerotiorum*. The use of specific antibodies directed against plant or fungal invertases revealed that much of the increase in activity could be attributed to a fungal isoform. In contrast to biotrophs, *S. sclerotiorum* triggers cell death (Dickman et al. 2001) and subsequently feeds as a saprophyte, which suggests that hexoses transported to the fungus are more likely the product of a fungal than a plant invertase. During infection, the acid invertase activity from plant origin did not support any increase and disappeared at the final stage of colonization, but a rise in fungal invertase expression was observed. During in vitro growth in the presence of sucrose, the fungal invertase was also produced and secreted in the culture medium. Voegele et al. (2006) reported on the appearance of a secreted fungal invertase during the

biotrophic interaction of *U. fabae* with *V. faba*. While sink associated plant invertases seem to be cell wall bound, this might not be the case for the respective enzymes provided by the pathogen. Involvement of fungal invertase in pathogenesis has only been demonstrated in the compatible biotrophic *V. faba/U. fabae* interaction (Voegele et al. 2006) and for the necrotrophic parasite *B. cinerea* (Ruiz and Ruffner 2002). Thus, our results contribute to establish that fungal invertase expression takes part to fungal plant pathogenesis and to the necrotrophic strategy of *S. sclerotiorum.*

Sucrose degradation and hexose sugar consumption were coordinated, as the expression of the hexose transporters genes *Sshxt1 and Sshxt2* reached maximal values 36 hpi, before decreasing at the latter stage of infection. Interestingly, levels of expression of *Sshxt1* and *Sshxt2* differed. *Sshxt2* was weakly expressed and was quantified as 20 times lower than *Sshxt1*. The wave patterns of expression exhibited by both transporters during infection could be related to specific ambient parameters created during infection. By lowering the ambient environmental pH, oxalic acid may affect the transcriptional regulation of pH-regulated genes necessary for pathogenesis and developmental life cycle of *S. sclerotiorum* (Cotton et al. 2003; Bolton et al. 2006). Extracellular hexose concentration is also a non-negligible control element. Glucose level reached 63 mM in healthy cotyledons, then 50 mM 48 hpi, which may favor the expression of low affinity hexose transporters. However, soluble intracellular sugars and hexoses released from cell wall and storage polymers degradation could be present, but inaccessible during the first hours of infection. As revealed by detection of a fungal invertase activity, sucrose degradation is actively performed until the end of infection and, consequently, should be correlated with a transport activity. The decreasing level of expression observed for both transporters 36 hpi, strongly suggests that additional transporters are necessary to support growth and development during the late stage of infection. Thus, a multiple transport system is likely to be expressed in *S. sclerotiorum* during pathogenesis. A screening for putative transporters-encoding genes revealed at least six additional sequences in the *S. sclerotiorum* genome. Candidate genes encoding, among others, homologues to sugar sensors (predicted to be high affinity transporters) or fructose transporters were revealed by the dendrogram. Therefore, *S. sclerotiorum* possesses a multigenic sugar transport system that could provide an efficient and flexible tool to this broad host range pathogen. Transcriptional analyses conducted during in vitro growth and functional characterizations of transporters should provide new insights on regulation, specificity and affinity of those transport proteins. The disappearance of sucrose in infected sunflower cotyledons, the expression of an invertase activity together with the expression of fungal hexose transporters are consistent with glucose and fructose being the sugars transferred from the host tissues to the pathogen. Even healthy parts of leaves also exhibited a loss of sugars, indicating that *S. sclerotiorum* was able to uptake nutrients from a distance.

During infection, strong modifications of NMR profiles reflecting the hydrolytic activity of the necrotroph were detected. The invasion of plant tissues was marked by an important rise of GPC and GPE levels, probably triggered by the attack of membrane polar lipids (Aubert et al. 1996). These data suggest that autolysis of the host membrane occurred. Fungal enzymes, such as phospholipases, are expressed during pathogenesis and could contribute to the degradation of these molecules (Lumdsen 1970). Moreover, these data are consistent with the behavior of *S. sclerotiorum* which is able to elicit host cell death and the fact that necrotrophic pathogens may need to trigger plant apoptotic pathway for successful colonization and subsequent disease development (Dickman et al. 2001).

The evolution in fungal trehalose and polyol contents was also followed during the course of infection. Trehalose, the second most abundant sugar accumulated in *S. sclerotiorum* mycelium, is a common storage product within microbial cell and especially in spores. Increased trehalose levels in fungi also have been correlated with cell survival under adverse conditions (Arguelles 1997). Trehalose was not accumulated during sunflower cotyledon infection and remained at a very low level. Infection-related development and colonization of host tissues could require the pathogen to mobilize storage carbohydrates. Trehalose mobilization has been involved in virulence-associated functions that follow host colonization in the pathogenic fungus *Magnaporthe grisea* (Foster et al. 2003). The absence of stored trehalose may also reflect a deviation of the fungal metabolites oriented toward an increased production of protective polyols such as glycerol. In filamentous fungi, polyols such as mannitol, glycerol, arabinitol and erythritol are widely distributed and can be accumulated to a high concentration (Jennings 1984). Their intracellular concentrations depend on growth conditions and developmental stages, suggesting that polyols have important functions in fungal physiology. Mannitol was the only polyol detected in the mycelium of *S. sclerotiorum* cultivated in vitro. It was produced by the fungus *in planta*. A fourfold increase was noticed in infected tissues from 24 to

48 hpi, whereas the amount of UDP-GlcNAc, that could reflect the evolution of the fungal biomass only doubled. Mannitol production, through the mannitol cycle (Jennings 1984) could be supplied by the degradation of sucrose from plant origin, particularly by an active conversion of fructose. Mannitol is considered as an important intermediate in the physiology of fungi (Jennings 1984). This hexilitol can be stored in fungal hyphae, or further metabolized in order to store reducing power or constitute a reserve carbon source (Ruijter et al. 2003). Secretion of mannitol is thought to directly protect invading pathogens by quenching host-produced reactive oxygen species (Jennings et al. 2002). In ectomycorrhizas, NMR spectroscopy investigations, to characterize carbohydrate metabolism during symbiotic state, revealed greater allocation of glucose to the synthesis of short chain polyols, whereas sucrose decreased in colonized roots (Martin et al. 1998). In the necrotrophic fungal pathogen *Stagonospora nodorum*, mannitol has been implicated in fungal plant interaction by revealing the incapacity of the mutant to sporulate *in planta* (Solomon et al. 2006). Levels of mannitol found in apoplastic fluids of infected leaves and in extracts of spores were observed to rise dramatically in the biotrophic interaction of the rust *U. fabae* with its host plant (Voegele et al. 2005). Thus, symbiotic or pathogenic interactions trigger similar metabolic responses, like an increase in mannitol production that could be a key regulatory component of carbon flow.

Contrary to mannitol, glycerol was not detected in *S. sclerotiorum* mycelium during in vitro growth, but it appeared in tissues from the first hours of infection. During the invasion process, glycerol increased by a factor of 5.4 from 24 to 48 hpi. By contrast, glycerol-3-P initially present in fungus and fairly abundant in the host plant, decreased during mycelium proliferation. Previous studies showed that, in plants, glycerol permeates all cell compartments and is phosphorylated very efficiently in the cytoplasm (Aubert et al. 1994). We have verified that sunflower cotyledons (healthy as well as infected) also phosphorylated an exogenous source of glycerol in a very efficient manner (data not shown). We therefore suggest that the glycerol observed in infected tissues was not localized in plant but was in the fungal hyphae during host plant invasion, where it was very likely synthetized and where it accumulated without permeating outside fungal hyphae. Subsequent modification of the fungal wall, like melanization, should render the hyphae non permeable to glycerol. For *M. grisea*, mechanical pressure derived from elevated osmotic pressure within melanized appressoria, through the accumulation of glycerol (Howard and Ferrari 1989). Melanization, which has been described in the sclerotial stroma of *S. sclerotiorum* (Bolton et al. 2006), could also be implicated in the modification of the infection hyphae. The amount of glycerol accumulated during infection was 4 times higher than that of mannitol, which characterized the mycelium during in vitro growth. During infection a metabolic switch could occur. Mannitol could be replaced by glycerol. However, the origin of this metabolic response remains to be elucidated. During *M. grisea* appressorium turgor generation, glycerol accumulation is a consequence of lipolysis (Wang et al. 2005). During the infection of sunflower cotyledons, glycerol could be a by-product of the degradation of lipids stored in germinations and subsequently accumulated by the fungus as a carbon storage compound. Alternatively, glycerol has also been reported as a compatible solute assuming osmotic stress protection necessary to maintain fungal cell expansion (Han and Prade 2002). We have observed that glycerol can abundantly accumulate in *S. sclerotiorum* under an osmotic stress provoked by addition of sodium chloride to the culture medium, while the mannitol content remained constant. Thus, glycerol could play a prominent role in osmostress adaptation. Osmoregulation during the course of pathogenesis has been demonstrated in the phytopathogenic fungus *C. fulvum.* In that case, arabinitol was the main polyol to respond to reduced water availability *in planta* and in vitro (Clark et al. 2003). Glycerol could play the same role in *S. sclerotiorum* where its accumulation could generate a turgor pressure essential for penetration of the fungus. As suggested by Voegele et al. (2005), conversion of carbohydrates taken up by the fungus into polyols would also maintain a gradient of metabolites toward the pathogen to support fungal development. Our results argue that metabolism and transport of soluble carbohydrates are of significance during plant pathogen interactions. During infection, the necrotrophic pathogen, *S. sclerotiorum* produces a drastic depletion of nutrients in plant tissues. The strong carbohydrate sink capacity of the fungus is linked to the presence of a multigenic hexose transport system and the expression of a fungal invertase during infection. Once transferred to the parasite, plant carbohydrates are likely to be converted in polyols. By enhancing penetration and draining capacities, accumulation of mannitol and glycerol *in planta* are likely to sustain the degradative strategy of *S. sclerotiorum.* The present study revealed the involvement of a fungal invertase during the necrotrophic pathogenesis of *S. sclerotiorum*, and the exclusive production of glycerol *in planta.* Molecular and biochemical analyses in these directions may help for

developing new knowledge about the pathogenesis of necrotrophic fungi.

Acknowledgments This work was supported by grants from the Ministère de la recherche, CNRS, the Université de Lyon, and the Région Rhône-Alpes. CJ was supported by a doctoral scholarship from the Région Rhône-Alpes. We thank AJ Dorne and MH Lebrun (Plant and Fungal Physiology, UMR 2847 CNRS-BayerCropScience, Lyon, France) for helpful comments. We are also indebt to JL Lebail for his dedicated technical assistance with the NMR spectrometer.

References

Abood JK, Lösel DM (2003) Changes in carbohydrate composition of cucumber leaves during the development of powdery mildew infection. Plant Pathol 52:256–265

Arguelles JC (1997) Thermotolerance and trehalose accumulation induced by the heat shock in yeast cells of *Candida albicans.* FEMS Microbiol Lett 146:65–71

Aubert S, Gout E, Bligny R, Douce R (1994) Multiple effects of glycerol on plant cell metabolism, phosphorus-31 nuclear magnetic resonance studies. J Biol Chem 269:21420–21427

Aubert S, Gout E, Bligny R, Marty-Mazars D, Barrieu F, Alabouvette J, Marty F, Douce R (1996) Ultrastructural and biochemical characterization of autophagy in higher plant cells subjected to carbon deprivation: control by the supply of mitochondria with respiratory substrates. J Cell Biol 133:1251–1263

Bago B, Pfeffer PE, Douds DD, Brouillette J, Bécard G, Shachar-Hill Y (1999) Carbon metabolism in spores of the arbuscular mycorrhizal fungus *Glomus intraradices* as revealed by nuclear magnetic resonance spectroscopy. Plant Physiol 121:263–271

Benhamou N, Grenier J, Chrispeels MJ (1991) Accumulation of ß-fructosidase in the cell walls of tomato roots following infection by a fungal wilt pathogen. Plant Physiol 97:739–750

Berger S, Papadopoulos M, Scheriber U, Kaiser W, Roitsch T (2004) Complex regulation of gene expression, photosynthesis and sugar levels by pathogen infection in tomato. Physiol Plant 122:419–428

Boland GJ, Hall R (1994) Index of plant hosts of *Sclerotinia sclerotiorum.* Can J Plant Pathol 16:93–108

Bolton MD, Thomma BPHJ, Nelson BD (2006) *Sclerotinia sclerotiorum* (Lib.) de bary: biology and molecular traits of a cosmopolitan pathogen. Mol Plant Pathol 7:1–6

Cabib E, Silverman SJ, Shaw JA, Das Gupta S, Park H-M, Mullins JT, Mol PC, Bowers B (1991) Carbohydrates as structural constituents of yeast cell wall and septum. Pure Appl Chem 63:483–489

Chen J, Saxton J, Hemming FW, Peberdy JF (1996) Purification and partial characterization of the high and low molecular weight forms (S-and F-form) of invertase secreted by *Aspergillus.* Biochim Biophys Acta 1296:207–218

Chou H-M, Bundock N, Rolfe SA, Scholes JD (2000) Infection of *Arabidopsis thaliana* with *Albugo candida* (white blister rust) causes a reprogramming of host metabolism. Mol Plant Pathol 1:99–113

Clark AJ, Blisset KJ, Oliver RP (2003) Investigating the role of polyols in *Cladosporium fulvum* during growth under hyperosmotic stress and in planta. Planta 216:614–619

Cotton P, Kasza Z, Bruel C, Rascle C, Fèvre M (2003) Ambient pH controls the expression of endopolygalacturonase genes in the necrotrophic fungus *Sclerotinia sclerotiorum*. FEMS Microbiol 227:163–169

Dickman M, Park Y, Oltersdorf T, Li W, Clemente T, French R (2001) Abrogation of disease development in plants expressing animal antiapoptotic genes. Proc Natl Acad Sci USA 98:6957–6962

Doehlemann G, Molitor F, Hahn M (2005) Molecular and functional characterization of a fructose specific transporter from the gray mold fungus *Botrytis cinerea.* Fungal Genet Biol 42:601–610

Foster AJ, Jenkinson JM, Talbot NJ (2003) Trehalose synthesis and metabolism are required at different stages of plant infection by *Magnaporthe grisea*. EMBO J 22:225–235

Fotopoulos V, Gilbert MJ, Pittman JK, Marvier AC, Buchanan AJ, Sauer N, Hall JL, Williams LE (2003) The monosaccharide transporter gene, *AtSTP4*, and the cell-wall invertase, *AtßfructI*, are induced in *Arabidopsis* during infection with the fungal biotroph *Erysiphe cichoracearum*. Plant Physiol 132:821–829

Godt DE, Roitsch T (1997) Regulation and tissue-specific distribution of mRNAs for the extracellular invertase isoenzymes of tomato suggests an important function in establishing and maintaining sink metabolism. Plant Physiol 115:273–282

Hall JL, Williams LE (2000) Assimilate transport and partitioning in fungal biotrophic interactions. Aust J Plant Pathol 27:549–559

Han K-H, Prade RA (2002) Osmotic stress-coupled maintenance of polar growth in *Aspergillus nidulans*. Mol Microbiol 43:1065–1078

Hegedus DD, Rimmer SR (2005) *Sclerotinia sclerotiorum*: when "to be or not to be" a pathogen? FEMS Microbiol Lett 251:177–184

Howard FJ, Ferrari MA (1989) Role of melanin in appressorium function. Exp Mycol 13:403–418

Jennings D (1984) Polyol metabolism in fungi. Adv Microbial Physiol 25:149–193

Jennings DB, Daub ME, Pharr DM, Williamson JD (2002) Constitutive expression of a celery mannitol dehydrogenase in tobacco enhances resistance to the mannitol-secreting fungal pathogen *Alternaria alternata.* Plant J 32:41–49

Joosten MHAJ, Hendrickx LJM, De Witt PJGM (1990) Carbohydrate composition of apoplastic fluids isolated from tomato leaves inoculated with virulent and avirulent races of *Cladosporium fulvum* (syn. *Fulvia fulva*). Neth L Plant Pathol 96:103–112

Laemmli UK (1970) Cleavage of structural proteins during the assembly of the head of the bacteriophage T4. Nature Lond 277:680–685

Lumdsen RD (1970) Phosphatidase of *Sclerotinia sclerotiorum* produced in culture and in infected bean. Phytopathology 60:1106–1110

Lumdsen RD, Dow RL (1973) Histopathology of *Sclerotinia sclerotiorum* infection of bean. Phytopathology 36:708–715

Madi L, McBride SA, Bailey LA, Ebbole DJ (1997) *rco-3*, a gene involved in glucose transport and conidiation in *Neurospora crassa.* Genetics 146:499–508

Marger MD, Saier MH (1993) A major superfamily of transmembrane facilitators that catalyse uniport, symport and antiport. Trends Biochem Sci 18:13–20

Martin F, Boiffin V, Pfeffer PE (1998) Carbohydrate and amino acid metabolism in the *Eucalyptus globulus Pisolithus tinctorius* ectomycorrhiza during glucose utilization. Plant Physiol 118:627–635

Maxwell DP, Lumdsen RD (1970) Oxalic acid production by *Sclerotinia sclerotiorum* in infected beans and in culture. Phytopathology 60:1395–1398

Mendgen K, Struck C, Voegele RT, Hahn M (2000) Biotrophy and rust haustoria. Physiol Mol Plant Pathol 56:141–145

Nehls U, Wiese J, Guttenberger M, Hampp R (1998) Carbon allocation in ectomycorrhiza: identification and expression analysis of an *Amanita muscaria* monosaccharide transporter. Mol Plant-Microbe Interact 11:167–176

Noeldner PKM, Coleman MJ, Faulks R, Oliver RP (1994) Purification and characterization of mannitol dehydrogenase from the tomato pathogen *Cladosporium fulvum* (syn. *Fulvia fulva*). Physiol Mol Plant Pathol 45:281–289

Özcan S, Johnston M (1999) Function and regulation of yeast hexose transporters. Microbiol Mol Biol Rev 63:554–569

Ratcliffe RG, Shachar-Hill Y (2001) Probing plant metabolism with NMR. Annu Rev Plant Physiol Plant Mol Biol 52:499–526

Riou C, Freyssinet G, Fèvre M (1991) Production of cell wall-degrading enzyme by the phytopathogenic fungus *Sclerotinia sclerotiorum*. Appl Environ Microb 57:1478–1484

Roberts JKM, Jardetsky O (1981) Monitoring of cellular metabolism by NMR. Biochim Biophys Acta 639:53–76

Roitsch T, Balibrea ME, Hofmann M, Proels R, Sinha AK (2003) Extracellular invertase: key metabolic enzyme and PR protein. J Exp Bot 382:513–524

Ruijter GJG, Bax M, Patel H, Flitter SJ, van de Vondervoort PJI, de Vries RP, vanKuyk PA, Visser J (2003) Mannitol is required for stress tolerance in *Aspergillus niger* conidiospores. Eukaryotic Cell 2:690–698

Ruiz E, Ruffner HP (2002) Immunodetection of *Botrytis*-specific invertase in infected grapes. J Phytopathol 150:76–85

Sambrook J, Fritsch EF, Maniatis T (1989) Molecular cloning: a laboratory manual. 2nd edn. Cold Spring Harbor Laboratory Press, Cold Spring Harbor, NY

Sato M, Muckler M (1999) A conserved amino acid motif (R-X-G-R-R) in the Glut1 glucose transporter is an important determinant of membrane topology. J Biol Chem 274:24721–24725

Scholes JD, Lee PJ, Horton P, Lewis DH (1994) Invertase: understanding changes in the photosynthetic and carbohydrate metabolism of barley leaves infected with powdery mildew. New Phytol 126:213–222

Shachar-Hill Y, Pfeffer PE (1996) Nuclear magnetic resonance in plant physiology. American Society of Plant Physiologists, Rockville, MD, pp 260–274

Sinha AK, Hofmann G, Köckenberger, Elling L, Roitsch T (2002) Metabolizable and non-metabolizable sugars activate different signal transduction pathways in tomato. Plant Physiol 128:1480–1489

Soanes DM, Skinner W, Keon J, Hargreaves J, Talbot NJ (2002) Genomics of phytopathogenic fungi and the development of bioinformatic resources. Mol Plant-Microbe Interact 15:421–427

Solomon PS, Waters ODC, Jörgens CI, Lowe RGT, Rechberger J, Trengove RD, Oliver RP (2006) Mannitol is required for sexual sporulation in the wheat pathogen *Stagonomosra nodorum.* Biochem J 399:231–239

Struck C, Mueller E, Martin H, Lohaus G (2004) The *Uromyces fabae UFAAT3* gene encodes a general amino acid permease that prefers uptake of *in planta* scarce amino acids. Mol Plant Pathol 5:183–189

Tang X, Rolfe SA, Scholes JD (1996) the effect of *Albugo candida* (white blister rust) on the photosynthetic and carbohydrate metabilosm of leaves of *Arabidopsis thaliana.* Plant Cell Environ 19:967–975

Towbin H, Staehelin T, Gordon J (1979) Electrophoretic transfer of proteins from polyacrylamide gels to nitrocellulose sheets: procedure and some applications. Proc Natl Acad Sci USA 76:4350–4354

Voegele RT, Struck C, Hahn M, Mendgen K (2001) The role of haustoria in sugar supply during infection of the broad bean by the rust fungus *Uromyces fabae*. Proc Natl Acad Sci USA 98:8133–8138

Voegele RT, Hahn M, Lohaus G, Link T, Heiser I, Mendgen K (2005) Possible roles for mannitol and mannitol dehydrogenase in the biotrophic plant pathogen *Uromyces fabae*. Plant Physiol 137:190–198

Voegele RT, Wirsel S, Möll U, Lechner M, Mendgen K (2006) Cloning and characterization of a novel invertase from the obligate biotroph *Uromyces fabae* and analysis of expression patterns of host and pathogen invertases in the course of infection. Mol Plant-Microbe Interact 19:625–634

Wang Z-Y, jenkinson JM, Holcombe LJ, Soanes DM, Veneault-Fourrey C, Bhambra GK, Talbot NJ (2005) The molecular biology of appressorium turgor generation by the rice blast fungus *Magnaporthe grisea.* Biochem Soc Trans 32:384–388

Wei H, Vienken K, Weber R, Bunting S, Requena N, Fischer R (2004) A putative high affinity hexose transporter *hxtA*, of *Aspergillus nidulans* is induced in vegetative hyphae upon starvation and in ascogenous hyphae during cleistothecium formation. Fung Genet Biol 41:148–156

Yu J, Chang P-K, Bhatnagar D, Cleveland TE (2000) Cloning of a sugar utilization gene cluster in *Aspergillus parasiticus.* Biochim Biophys Acta 1493:211–214

Zdobnov EM, Apweiler R (2001) "InterProScan-an integration platform for the signature-recognition method in InterPro". Bioinformatics 17:847–848